

CADNet: A lightweight Neural Network for Coronary Artery Disease Classification Using Electrocardiogram Signals

Atitaya Phoemsuk, and Vahid Abolghasemi

Abstract—Coronary Artery Disease (CAD) is characterised by a diminished capacity of the coronary arteries to supply sufficient blood, oxygen and nutrients to the heart. It primarily develops due to the presence of fat deposits and arterial plaques, and it is a leading cause of global mortality. Given the limited accessibility, high cost, and inconvenience of invasive diagnostic tools, we propose a lightweight one-dimensional convolutional neural network for CAD classification using non-invasive electrocardiography (ECG) signals. The proposed model, CADNet, consists of two key components: Feature Encoding and Compact Pooling. The feature encoding block extracts key temporal characteristics from ECG data using a convolutional layer, while the compact pooling block reduces temporal resolution, preserving essential ECG features for CAD diagnosis. CADNet comes with a novel data purification process to optimise computational efficiency and maintain high diagnostic accuracy. This approach aids convergence, significantly reduces the model parameters, and improves the model's ability to detect CAD patterns. Our extensive experiments with four diverse datasets show that CADNet achieves an average 99.3% accuracy, with 2,586 trainable parameters, surpassing state-of-the-art models performance.

Index Terms—Cardiovascular diseases, Coronary Artery Disease, Convolutional Neural Network, Electrocardiogram.

I. INTRODUCTION

A. Overview

Coronary Artery Disease (CAD), involving the left anterior descending artery, is increasingly observed in young adults, driven by factors such as elevated cholesterol levels, hypertension, and tobacco use [1]. This condition typically presents as single-vessel disease rather than multi-vessel involvement. CAD continues to be a leading cause of mortality among individuals aged 35 and older across both developed and developing nations [2]. CAD develops when the supply of oxygen-rich blood to the heart muscle is restricted or impeded, placing increased strain on the heart. This condition can lead to various clinical outcomes, such as angina—chest pain resulting from restricted blood flow to the heart muscle, heart attacks, which occur when blood flow to the heart muscle is suddenly blocked, and heart failure, where the heart is unable to pump blood throughout the body effectively. CAD

represents one subtype of cardiovascular diseases (CVDs), which remains the leading cause of mortality globally. The World Health Organisation (WHO) report highlights that in 2023, CVDs were responsible for approximately 17.9 million deaths globally, representing 32% of all worldwide fatalities [3]. Of these deaths, 85% were attributed to heart attacks and strokes, with a primary occurrence in low- and middle-income countries, which accounted for over three-quarters of such deaths. Therefore, early diagnosis is imperative in preventing many CVDs and addressing behavioural risk factors. This proactive approach aids in reducing both mortality rates and the prevalence of individuals unaware of their medical conditions [4]. Moreover, implementing cost-effective diagnostic tools is necessary for achieving early diagnosis and raising awareness of medical conditions among patients.

B. Related works

Currently, Angiography is a popular tool for CVDs screening; however, its use in patient follow-up and treatment is restricted due to its invasive nature, high cost, and the need for substantial technical expertise. With the advancement of state-of-the-art technologies, low-cost diagnostic tools are being introduced through research by leveraging artificial intelligence (AI). Electrocardiography (ECG) is the primary method used for initial screening of CVDs in general medical practices. General practitioners rely on recorded ECGs as essential diagnostic tools in their evaluation process. In diagnosing CVDs, a comprehensive understanding of risk factors and sound medical expertise is crucial to enhance diagnostic accuracy. Additionally, it is frequently employed as a preliminary screening tool in general medical practices due to its capability for continuous non-invasive monitoring and real-time data provision [5].

Although ECG proves to be an effective diagnostic tool by recording the heart's electrical activity, the current diagnostic procedures involving ECG are dominantly performed manually by practitioners and doctors, which is time-consuming and prone to errors. The development of state-of-the-art technologies has led to the introduction of various automated systems for diagnosing CVDs, aiming to tackle these identified difficulties [6]–[8]. However, such explorations have been underrepresented in CAD diagnosis. Hence, developing automated ECG-based diagnosis is becoming increasingly crucial in modern healthcare, primarily due to the limitations of manual diagnosis methods. Automated diagnosis can be facilitated

A. Phoemsuk and V. Abolghasemi are with the School of Computer Science & Electronic Engineering, University of Essex, UK, CO4 3SU, emails: {ap19698,v.abolghasemi}@essex.ac.uk

by applying AI algorithms to learn from large amounts of data and provide accurate diagnostic results without the need for expertise. Furthermore, automated diagnostic systems could offer convenience to both patients and practitioners.

Traditional machine learning (ML) techniques, such as Support Vector Machine (SVM), K-nearest Neighbours (kNN), K-means, and Decision trees, have been extensively utilised in ECG analysis for diagnosing various cardiac conditions. SVM is applied in ECG analysis not only for diagnosing CAD [9] but also for detecting various other cardiac conditions, including atrial fibrillation (AF) [10]–[12], arrhythmia [13]–[15], and myocardial infarction (MI) [16]. Furthermore, kNN algorithm has attracted considerable attention from researchers for its efficacy in classifying ECG data, particularly in diagnosing arrhythmia, AF and CAD [17]–[20]. ML-based algorithms heavily depend on efficient feature extraction processes, given that the quality of the ECG data can profoundly influence the performance of the model. The effectiveness of hand-crafted feature extraction methods in capturing relevant ECG features may vary depending on the complexity and variability of the data, potentially leading to decreased model performance and diagnostic accuracy. As a result, the application of ML-based models may require considerable time due to the necessity of feature extraction, in contrast to deep learning (DL) methodologies.

The limitations of feature extraction methods in traditional ML prompt exploration into alternative methodologies for ECG diagnosis. DL-based algorithms, including Convolutional Neural Networks (CNN) [7], [8], [21], Recurrent Neural Networks (RNN) [22], [23], Long-short term memory (LSTM) [24], have been introduced for CAD diagnosis. The primary advantage of DL-based methods is their ability to eliminate the need for feature extraction, as these models can learn directly from large amounts of data and effectively diagnose ECG-related issues. In recent years, CNN-based models have been applied not only to image data but have also been introduced by researchers to analyse time-domain data such as ECG. It offers the capability to automatically learn discriminative features directly from raw ECG signals, thus, eliminating the need for hand-crafted feature extraction and enabling the capture of complex temporal patterns inherent in ECG data. This focus on automated feature extraction aligns with recent advancements in other biomedical domains [25], where a Variational Gated Autoencoder (VGAE) has been utilised to extract latent features from multiview biomedical data. This approach illustrates the potential of deep learning-based architectures to effectively manage complex, high-dimensional datasets, offering insights that may be applied to ECG analysis. In [26], CNN-based models have significantly advanced ECG signal processing by enabling automatic and hierarchical feature extraction. In contrast to traditional approaches, which rely on handcrafted features, CNN learns complex patterns directly from raw ECG data. This capability not only reduces reliance on manual feature engineering but also enhances robustness to noise and variability.

Deep learning models typically require significant computational power and resources, making them unsuitable for devices with limited capabilities. This limitation motivates

the development of lightweight models designed to minimise computational and memory requirements. The application of lightweight CNNs for ECG signal classification has gained significant attention in recent years, primarily in the context of arrhythmia detection. These models enable efficient operation on resource-constrained devices, offering advantages such as faster inference times and lower energy consumption, which are crucial for real-time diagnosis. A study by Mewada [27], proposed a 2D-wavelet encoded deep CNN for ECG classification, transforming one-dimensional ECG signals into two-dimensional representations to incorporate spatial feature extraction capabilities. The author demonstrated that their approach improved arrhythmia detection accuracy without the need for extensive preprocessing. Similarly, another work examined lightweight CNN models applied to ECG datasets, emphasising the reduction of computational complexity while maintaining high classification performance for arrhythmias [28]. These approaches focus primarily on detecting abnormal heart rhythms, which are largely associated with electrical malfunctions in cardiac activity. Further, a study investigating lightweight CNN architectures specifically for ECG signal classification showcased the effectiveness of optimised deep learning models in diagnosing arrhythmic events [29]. Additionally, researchers explored efficient CNN architectures to enhance real-time arrhythmia classification, optimising neural network layers to improve model interpretability and deployment in clinical environments [30]. In [31], a lightweight CNN for MI diagnosis was introduced, aiming to minimise computational and storage demands to facilitate deployment on portable devices. Utilising the Physikalisch Technische Bundesanstalt (PTB) diagnostic database, various baseline CNN configurations were evaluated and compared to their proposed lightweight model. Results indicated that the proposed model maintained high accuracy while reducing model complexity. Several lightweight networks have been utilised for ECG analysis, including SqueezeNet [32], EfficientNet [33], MobileNet [34], and ShuffleNet [35]. These widely well-established models are specifically designed for deployment on resource-constrained devices, enabling efficient applications in such environments. In a notable advancement in novel technology, an ultra-lightweight end-to-end electrocardiogram classification neural network has been developed. The research employed advanced techniques aimed at reducing computational complexity while maintaining high-performance standards, making it suitable for integration into portable and wearable medical devices [36].

While these studies contribute valuable insights into the detection of arrhythmias, they do not directly address the challenges associated with coronary artery disease diagnosis. Unlike arrhythmias, which often present distinct electrical anomalies, CAD is characterised by subtle ischemic patterns and morphological changes in ECG signals. The detection of CAD requires domain-specific adaptations that extend beyond the capabilities of conventional arrhythmia-focused CNN models. In this study, we propose a lightweight one-dimensional convolutional neural network (CADNet) for automated CAD diagnosis. Our research distinguishes itself by targeting CAD classification, which presents unique challenges in early de-

tection due to the absence of overt electrical abnormalities. We propose an advanced lightweight CNN framework that integrates specialised feature extraction techniques to identify ischemic patterns in ECG signals. By tailoring the model architecture to CAD-specific markers, we aim to improve diagnostic accuracy while ensuring computational efficiency for real-time deployment.

Compared with other existing lightweight models, deep learning-based models and traditional machine learning algorithms, our model demonstrates advantages in terms of reduced model size while maintaining high accuracy. This important capability facilitates the deployment of CADNet in clinical settings. This is particularly significant because traditional deep learning models require substantial computational resources, making them unsuitable and costly for real-time diagnosis and deployment on portable devices.

C. Our contributions

CADNet introduces several key innovations specifically tailored for coronary artery disease (CAD) detection, addressing challenges that conventional arrhythmia-focused CNN models often overlook.

- 1) Innovative Data Purification Module: We introduce a novel data refinement process that combines sample entropy and standard normalisation, improving signal quality and computational efficiency before classification. This significantly enhances the reliability of CAD diagnosis.
- 2) Specialised for CAD Detection: Unlike arrhythmia classification, which often relies on clear electrical anomalies, CAD detection requires identifying subtle ischemic patterns in ECG signals. Our model incorporates domain-specific adaptations to improve sensitivity to these patterns, which are often overlooked by traditional CNN models.
- 3) Lightweight Yet High-Performing Architecture: CADNet achieves 99.3% accuracy with only 2,586 trainable parameters, significantly reducing computational overhead. This ensures its feasibility for real-time deployment in resource-constrained environments, an area where many existing deep learning models struggle due to high computational demands.
- 4) Novel Architectural Enhancements: Feature Encoding Block: Optimised convolutional layers to capture temporal characteristics relevant to CAD.
- 5) Compact Pooling Block: A new pooling strategy designed to retain essential ECG features while improving computational efficiency.
- 6) Comprehensive Benchmarking and Generalisation: We rigorously evaluated CADNet across four diverse datasets (PTB-XL, MIMIC-III, St. Petersburg, Fantasia), demonstrating superior accuracy and robustness. Additionally, we assessed its performance across different age groups to confirm its generalisability.

D. Outline

The remainder of this paper is structured as follows. Section II details the proposed methodology, including data preparation, purification, model architecture and optimisation. Section III describes the experimental setup, performance metrics, datasets, and results and discussions. Section IV is devoted to drawing limitations and future directions of this research. Finally, Section V concludes the paper.

II. MATERIALS AND METHODS

This section outlines different steps for comprehensive CAD classification using our proposed CADNet model. Figure 1 illustrates the process of classifying binary classes, i.e. CAD and non-CAD, from ECG data. The process initiates with raw ECG signals, obtained from the MIMIC III, Fantasia, St Petersburg and PTB-XL databases. For training, the ECG signals are meticulously chosen from MIMIC III and Fantasia databases, partitioned into 1-second segments and categorised into subsets, as outlined in Section ???. For testing, the same procedure is followed but using St Peterburg and PTB-XL databases. A novel data purification technique is then applied to the subsets to eliminate noise and irrelevant data (Section II-B). The proposed CADNet model (described in Sections II-D and II-C) is subsequently employed to classify the ECG signals as either indicative of CAD or non-CAD.

A. Data preparation

1) *Data source*: The ECG data used in this study are sourced from four publicly available databases accessible through PhysioNet: MIMIC-III [37], St. Petersburg [38], PTB-XL [39] and Fantasia [40]. The details of each dataset are outlined below:

a) *MIMIC-III*: The MIMIC-III dataset includes a total of 2,840 patients diagnosed with coronary atherosclerosis in the native coronary artery, accounting for approximately 7.1% of total hospital admissions. ECG recordings from these patients were extracted and utilised for analysis.

b) *St. Petersburg*: This dataset consists of 30-minute ECG recordings from 75 subjects, among whom 7 patients have been diagnosed with CAD. The ECG signals from these patients were selected for this study.

c) *PTB-XL*: PTB-XL is a large-scale ECG dataset containing over 20,000 10-second recordings from approximately 18,000 patients. This dataset includes a variety of cardiac conditions, providing essential subclasses that support CAD diagnosis.

d) *Fantasia*: The Fantasia dataset consists of ECG recordings from a cohort of 40 individuals, evenly distributed between 20 young and 20 adult subjects. This dataset was used to represent non-CAD patients in our study.

2) *Data preprocessing and segmentation*: ECG recordings from CAD and non-CAD patients were selected from each database and segmented into one-second ECG data segments, each comprising $N = 250$ samples. A similar data selection strategy was used in [24], where ECG recordings from the Fantasia and St. Petersburg databases were used to represent

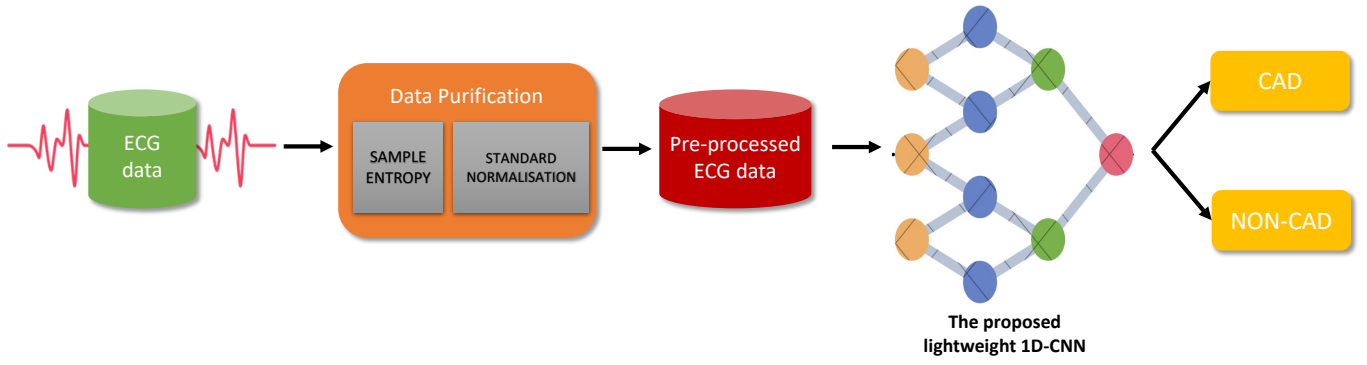


Fig. 1: Flowchart outlining the operational framework of the proposed model

normal and CAD subjects, respectively. This segmentation method enables detailed analysis of the dynamic variations and patterns in ECG signals within short temporal windows. Such an approach has been widely used to maintain consistency in ECG signal analysis [24], [41], [42], as it captures the ECG cycle without relying on waveform detection methods. Following segmentation, a data purification process (explained in the next subsection) was applied to remove irrelevant noise within the ECG segments. To facilitate classification, a binary label was assigned to each sample:

- Label 0: Non-CAD subjects from the Fantasia database.
- Label 1: CAD-diagnosed subjects from the MIMIC-III, St. Petersburg, and PTB-XL datasets.

3) *Dataset composition for training and evaluation*: A primary subset comprising 200 ECG signals was created for training and testing. The dataset maintains an equal distribution of CAD and non-CAD subjects, with 100 ECG signals sourced from the MIMIC-III and Fantasia databases. To ensure robust evaluation, we employed ten-fold cross-validation, a widely used technique in both traditional machine learning and deep learning. For each fold, the dataset was split 70% for training and 30% for testing. To mitigate overfitting, dropout and early stopping strategies were implemented. Training was terminated if no improvement in validation loss was observed over eight consecutive epochs.

B. Data purification

Since biomedical data are normally recorded with many unwanted noises and artifacts, proper data purification would play a pivotal role in ensuring the quality and consistency of input data (ECG here). And, the signal quality notably influences the model's performance [43], [44]. Consequently, researchers consider implementing various pre-processing techniques to ensure optimal accuracy.

Sample entropy emerges as a prominent method within temporal data applied in previous studies to enhance signal quality [45], [46]. Unlike standard entropy or approximate entropy, sample entropy provides a more consistent and robust estimate of signal complexity, especially in shorter and noisier time-series signals, which are common in real-world ECG recordings. Here, we propose a data purification technique, based on sample entropy, to facilitate CAD classification,

combining the sample entropy concept and a standard normalisation step. In CADNet, this combination is applied to the raw ECG data to mitigate artifacts present in the signal. Sample entropy functions as a metric to evaluate the time series data quality. Additionally, standard normalisation is applied to eliminate flat time series data and mitigate any potential influences that could affect the model's accuracy. Sample entropy is mathematically defined as:

$$SampEn = -\ln \left(\frac{\sum_{i=1}^{N-m} Q_i^m(r)}{\sum_{i=1}^{N-m+1} P_i^{m+1}(r)} \right) \quad (1)$$

where $SampEn$ indicates the quality of the ECG signals. N signifies the quantity of samples within each 1-second segment of the ECG. m denotes the embedded dimension, which indicates the length of consecutive samples or data points analysed jointly, with $m = 2$. r denotes the tolerance threshold, which defines the acceptable range of similarity between points, enabling the identification of meaningful patterns in the ECG data while maintaining robustness to noise. In our study, we set $r = 0.1$, a value supported by previous research, where r values between 0.1 and 0.25 are effective in maintaining signal quality in ECG data [47]. $Q_i^m(r)$ quantifies the instances of vector pairs of dimension m whose mutual distance falls below r , suggesting a degree of similarity or regularity within the signal. $P_i^{m+1}(r)$ measures the quantity of vector pairs with dimension $m + 1$ demonstrating similarity within the predetermined threshold r , thereby expanding the comparison to sequences of extended length.

Following applying the $SampEn$, the retained ECG signals undergo standard normalisation to remove any remaining flat and noisy artifacts:

$$\sigma = \sqrt{\frac{1}{N-1} \sum_{i=1}^N (x_i - \bar{x})^2}. \quad (2)$$

In (2), σ represents the quality of the ECG signals, N denotes the quantity of signals, \bar{x} signifies the average of a given signal, and x_i denotes the signal value at the i^{th} position.

Fig. 3 illustrates examples of ECG signals evaluated during the data purification process. Fig. 3(a) shows a high-quality signal exhibiting appropriate morphological complexity and variance, with a $SampEn$ below 0.1 and a standard deviation

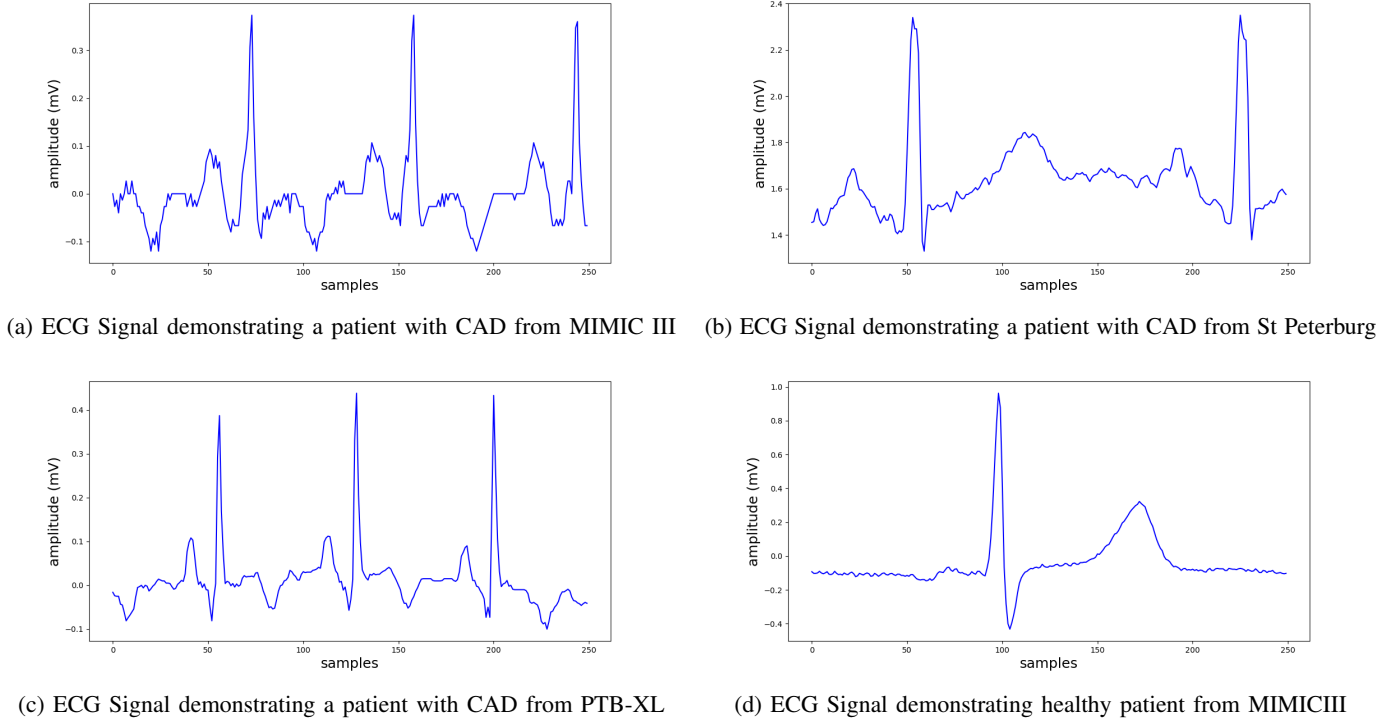


Fig. 2: Example of ECG signals from different databases used (MIMIC III, St Petersburg and PTB-XL)

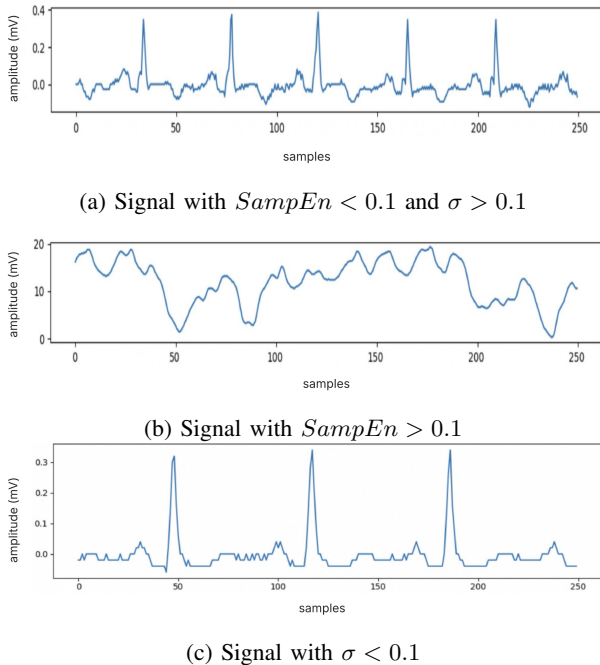


Fig. 3: Examples of ECG signals during the data purification process. Signals with $SampEn < 0.1$ were considered to exhibit appropriate complexity, while a standard normalisation threshold of $\sigma > 0.1$ was used to exclude flat signals. Only ECG signals satisfying both criteria were retained for further analysis.

σ above 0.1. Fig. 3(b) presents a signal with $SampEn > 0.1$, likely due to noise or random fluctuations. Fig. 3(c) shows a signal exhibiting flatness, with a $\sigma < 0.1$. Only signals that met both criteria were used for further analysis.

To further quantitatively evaluate the impact of data purification, the average Root Mean Squared Error (RMSE) was calculated between the original ECG signals and the processed ECG signals after the data purification process, for both CAD and non-CAD cases. The RMSE was 3.66 for CAD and 4.26 for non-CAD signals. These relatively low values suggest that the data purification step effectively removed inappropriate ECG segments while preserving the overall ECG waveform structure. The slightly higher RMSE in the non-CAD cases may be due to the more regular and stable patterns typically found in healthy ECG signals, which can be more easily removed during the data purification. However, this does not compromise the model’s ability to learn from the ECG signals. Visual inspection confirmed that key clinical components, such as the P-wave, QRS complex, and T-wave, remained clearly visible.

C. Lightweight deep learning architecture

Figure 4 illustrates the operational framework of our CAD-Net model. It is a lightweight 1D-CNN designed for efficient and effective CAD detection and optimises computational resources while delivering robust performance in a CAD classification task. The proposed CADNet model consists of two main blocks: Feature Encoding and Compact Pooling layers. These components enhance the model’s robustness to

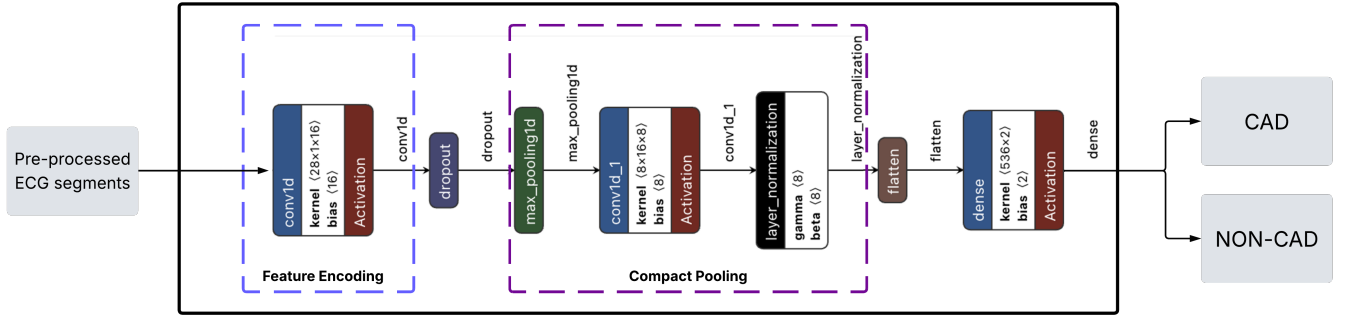


Fig. 4: Detailed architecture of the proposed CADNet including feature encoding, compact pooling and classification blocks.

noise and fluctuations in ECG signals, thereby improving its ability to classify CAD with precision and efficiency. The fully connected layer comprises two neurons and utilises Softmax activation, facilitating the classification of the input ECG signal into one of two potential classes, thereby representing the probabilities of the input belonging to each class. Furthermore, a dropout layer is incorporated between the primary blocks to augment the model’s capacity for generalisation.

Feature Encoding block plays a crucial role in transforming raw ECG input data into a higher-dimensional feature space, efficiently capturing critical temporal patterns while minimizing dimensionality. This layer preserves essential diagnostic characteristics, including P waves, QRS complexes, and T waves, facilitating the efficient extraction of significant ECG features with minimal computational cost. This block is a convolutional layer consisting of 16 filters. Each filter is responsible for identifying specific patterns or features within ECG data. The kernel size for each filter is set to 28. Consequently, during each convolution operation, the filter examines a window of 28 consecutive ECG samples from the ECG signal. This approach enables the filter to capture local patterns or features within the ECG signal that may indicate particular cardiac events or abnormalities of CAD. ReLU activation functions are employed within the block for their simplicity and computational efficiency. These functions introduce non-linearity to the model, facilitating the learning of complex patterns in the data while managing computational capacity effectively. The output of the feature encoding layer is calculated as:

$$y_i = \sum_{k=1}^K x_{i+h-1} \cdot w_h + b \quad (3)$$

where y_i represents the output signal at position i -th position within the feature encoding layer. K denotes the number of weights within the filter, determining the size of the window that slides the input ECG signal. x_{i+h-1} represents each element of the ECG input aligned with a specific weight in the filter, denoted by w_h , during the computation of the output signal at i position. The bias term, represented by b , is initialised to zero. This initialisation enables the model to achieve greater flexibility in fitting the ECG data by adjusting the activation function.

The compact pooling layer is employed to reduce the

temporal resolution of the ECG signals, refine the extracted features, and ensure that only the most relevant information for classification is passed to subsequent layers. This layer comprises max pooling, convolutional, and layer normalisation layers. The max pooling layer is introduced to operate within sliding windows of size 3, effectively reducing the temporal resolution of the signal while preserving essential temporal ECG features. Subsequently, a one-dimensional convolutional layer with a filter size and kernel size of 8 each is employed. The Rectified Linear Unit (ReLU) activation function is then applied to facilitate the detection of complex patterns indicative of CAD. Finally, layer normalisation is used to ensure promoting convergence and enhancing the model’s ability to discern relevant CAD patterns in the ECG data. The layer normalisation can be computed via:

$$y_i = \gamma \left(\frac{x_i - \mu}{\sqrt{\sigma^2 + \epsilon}} \right) + \beta \quad (4)$$

where y_i represents the output signal of the normalisation layer for the i -th position. Learnable parameters denoted by γ and β , respectively. x_i indicates the input signal at i -th position. μ represents the average of the input signal. σ^2 denotes the variability or dispersion of ECG features, where ϵ would be a small constant added to the denominator for numerical stability, ensuring that the denominator is never zero or too close to zero during computations.

D. Optimisation

The model is trained using binary cross-entropy loss, the Adam optimiser, ReLU and Softmax activation functions. The hyperparameters employed during model training, including learning rate, batch size, and number of epochs, are provided in Table I. A binary cross-entropy (BCE) loss function is employed for CAD and non-CAD classification purposes due to its effectiveness in handling binary classification tasks:

$$\text{BCE} = -\frac{1}{N} \sum_{i=1}^N (y_i \log(p_i) + (1 - y_i) \log(1 - p_i)) \quad (5)$$

where N represents the total number of samples contained within the respective ECG segment. y_i denotes the actual label assigned to ECG signals i , where $y_i \in \{0, 1\}$. $y_i = 0$ corresponds to a non-CAD case, indicating the absence

TABLE I: Hyperparameters used for model training

Hyperparameter	Value
Learning Rate	0.0001
Batch Size	32
Number of Epochs	50
Optimiser	Adam
Loss Function	Binary Cross-Entropy
Hidden Layer Activation	ReLU
Output Layer Activation	Softmax

of CAD features within ECG signal i . Conversely, $y_i = 1$ indicates a CAD case, signifying the presence of relevant CAD characteristics in ECG signal i . p_i denotes the anticipated probability that ECG signal i is associated with class 1. It assists the model in determining the accuracy of its predictions, thereby facilitating adjustments to enhance its predictive capability to align more closely with the actual labels.

Adam optimiser was utilised to enhance the efficacy of training our CADNet, employing a learning rate of 0.0001. Its capability to dynamically adjust learning rates for individual parameters ensures proficient optimisation, accommodating the nuanced gradients inherent within ECG data.

ReLU activation function, a key component of convolutional layers due to its simplicity and effectiveness, is presented via:

$$\text{ReLU}(x) = \max(0, x) \quad (6)$$

where an ECG input signal represented by a vector $x = [x_1, x_2, \dots, x_n]$. ReLU transforms negative inputs to zero while preserving positive inputs, rendering it computationally efficient and ensuring differentiability across its domain, except at zero. This capability facilitates the network in capturing intricate patterns and features inherent in ECG data.

III. EXPERIMENTAL RESULTS

Extensive experiments were conducted to evaluate the performance of the proposed model. A machine equipped with an Apple M2 Max processor and 32 GB of unified memory was used to run all the experiments. The implementation was carried out using Python 3.9.6. We also provide comparative analyses with classical machine learning algorithms, existing DL-based models, and well-known lightweight models. Table I summarises the hyperparameters used in our experiments.

A. Performance metrics

In this study, standard classification metrics were employed, namely accuracy (Acc), precision (Ppr), Sensitivity (Sen), Specificity (Spr), and F1 Score ($F1$) for evaluating the classification performance. These metrics were explicitly defined as follows:

$$Acc = \frac{TP + TN}{TP + TN + FP + FN} \quad (7)$$

$$Ppr = \frac{TP}{TP + FP} \quad (8)$$

$$Sen = \frac{TP}{TP + FN} \quad (9)$$

$$Spr = \frac{TN}{TN + FP} \quad (10)$$

$$F1 = \frac{2 \times Sen \times Ppr}{Sen + Ppr} \quad (11)$$

where True Positives (TP) are the CAD cases that the model correctly identifies as CAD, True Negatives (TN), are the non-CAD cases correctly identified as non-CAD, False Positives (FP) are the non-CAD cases mistakenly identified as CAD, and False Negatives (FN) are the CAD cases mistakenly identified as non-CAD.

Furthermore, Area Under Curve (AUC) was utilised to quantify the model's ability to differentiate between CAD and non-CAD cases as shown in (12).

$$AUC = \sum_{i=1}^{n-1} \frac{1}{2} \cdot (FPR_{i+1} - FPR_i) \cdot (TPR_i + TPR_{i+1}) \quad (12)$$

where:

$$FPR = \frac{FP}{FP + TN} \quad (13)$$

and FPR_i signifies the percentage of cases without CAD that are inaccurately classified as having CAD at the i^{th} threshold. TPR_i (Sen) represents the proportion of cases with CAD that are correctly identified as having CAD at the i^{th} threshold. n is the total number of thresholds. $FPR_{i+1} - FPR_i$ is the difference in the proportion of cases without CAD that are incorrectly identified as having CAD between two consecutive thresholds. $TPR_{i+1} - TPR_i$ demonstrates the total proportion of individuals with CAD correctly identified as having CAD at the two consecutive thresholds.

Additionally, t-distributed Stochastic Neighbour Embedding (t-SNE) analysis is carried out to visualise high-dimensional feature representations in a two-dimensional space, offering insights into the ability of each key module within the CADNet model to differentiate between classes. The t-SNE equation is defined as follows:

$$KL(P \parallel Q) = \sum_i \sum_{j \neq i} p_{ij} \log \frac{p_{ij}}{q_{ij}} \quad (14)$$

where p_{ij} and q_{ij} denote the joint probabilities of a pair of ECG data points, i and j , in the high-dimensional feature space and the corresponding low-dimensional space, respectively.

B. Ablation study

Table II provides an ablation study to systematically evaluate the effectiveness of different developments we applied to the baseline 1D-CNN to finally propose the CADNet model. As found from Table II, the baseline 1D-CNN model achieved a high accuracy of 99.3%, requiring approximately 8 million trainable parameters, a size of 32,190 KB, and a runtime of 854.8449 seconds. This highlights its substantial complexity, runtime demands, and storage and computational requirements, making it computationally intensive and unsuitable for

TABLE II: Ablation analysis among the baseline 1D-CNN model and different layers of the proposed CADNet.

Model Architecture	Trainable params	Size	Acc (%)	Run time (s)
Baseline 1D-CNN	8,439,426	32.19 MB	99.3	854.8449
Feature Encoding layer	8,552	33.41 KB	97.8	5.0911
Feature Encoding layer + Compact Pooling layer	2,586	10.10 KB	98.5	8.3467
CADNet: Feature Encoding layer + Compact Pooling layer + Dropout	2,586	10.10 KB	99.3	10.0856

resource-constrained environments, such as wearable devices or real-time monitoring systems. To address this limitation, we developed a lightweight model through a feature encoding layer. This new architecture reduces the trainable parameters to 8,552, with a size of 33.41 KB, while reducing the accuracy to 97.8% (Table II). This suggests that the feature encoding layer could significantly lower parameters at a price of a slight reduction in accuracy compared to the baseline 1D-CNN. To further improve the model performance, the feature encoding layer and compact pooling were integrated to attempt a further reduction in the number of trainable parameters while maintaining accuracy. The integration of these two layers successfully reduced the number of trainable parameters and size (Table II). We have implemented several robust regularisation techniques in our proposed CADNet architecture to avoid overfitting. Specifically, we have employed:

- **Dropout tuning:** We have incorporated dropout layers within our model architecture. By randomly deactivating neurons during training, these layers reduce the model's dependency on any single feature, thereby enhancing its ability to generalise to unseen data.
- **Early stopping:** To further mitigate overfitting, we applied an early stopping mechanism. Training is terminated if no improvement in the validation loss is observed over eight consecutive epochs. This prevents the model from training excessively on the training data and helps in avoiding overfitting.
- **Model efficiency:** As detailed in Table II, CADNet features a minimal number of trainable parameters and a compact storage size, which naturally limits the model's capacity to overfit. Despite these constraints, our model achieved an accuracy of 99.3% and maintained a runtime of 10.0856 seconds, making it highly suitable for real-time CAD diagnosis in devices with limited computational resources.

As a result, the model becomes less sensitive to noise in the training set, enabling it to better generalise to unseen samples. The proposed CADNet (Table II) ultimately featured a minimal number of trainable parameters and compact storage size, while maintaining a high level of accuracy at 99.3% with a shortest runtime of 10.0856 seconds, making it suitable for real-time CAD diagnosis. This significant improvement ensures its feasibility for devices with limited computational resources, bridging the gap between high performance and practical applicability.

C. Computational analysis

Figure 5 indicates the impact of each proposed architecture in reducing the number of trainable parameters. The baseline

model was able to achieve an overall classification accuracy of 99.3%. However, the number of trainable parameters remains notably high, indicating significant computational demands. It can be observed that as the proposed feature encoding, compact pooling, and dropout layers are successively added, the number of trainable parameters decreases from approximately 8 million to 8,552, 2,586, and 2,586, respectively. Remarkably, even as the model becomes more streamlined with fewer parameters, its performance remains consistently high, maintaining high accuracy. This observation underscores the effectiveness of the proposed techniques in optimising the model's complexity without compromising its predictive capability.

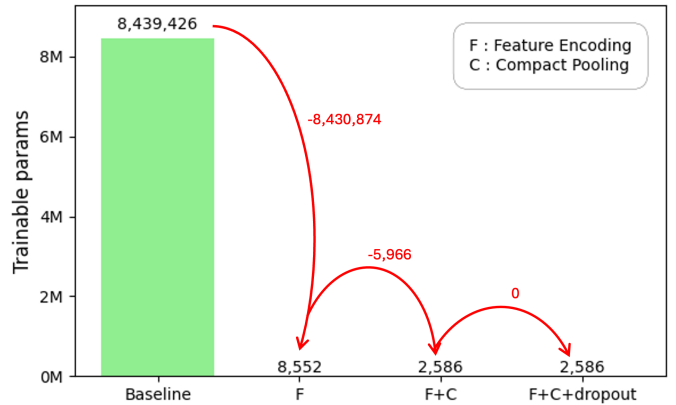


Fig. 5: Comparison of parameter meter analysis between the established CNN model and our proposed lightweight model. The chart illustrates the key metrics derived from the analysis, showcasing the efficiency and effectiveness of our proposed model in terms of parameter utilisation.

D. Comparative study

Table III illustrates a comparison among different traditional ML-based, DL-based network and lightweight network architectures. Additionally, it highlights differences in model size and runtime across various architectures, providing insights into their computational efficiency and potential suitability for resource-constrained environments. The models are evaluated based on trainable parameters, file size, runtime and performance metrics including *Acc*, *AUC*, and *F1* score. The classical ML-based methods applied to our subset include SVM, Gaussian Naive Bayes, K-Means, KNN, and Logistic Regression. The various DL-based models we compared include LSTM, CNN-LSTM, RNN, and a baseline 1D-CNN. Moreover, well-known lightweight networks, including

TABLE III: Comparative analysis of traditional ML-based, DL-based and lightweight networks utilising ten-fold cross-validation.

Model Architecture	Trainable params	Size (KB)	Acc (%)	AUC (%)	F1 score (%)	Runtime (s)	Inference time(ms)
SVM	0	38.72	83.5	82.5	83.1	0.7087	0.0527
Gaussian Naive Bayes	0	8.41	92.4	98.7	92.4	0.0039	0.0419
KNN	0	353.66	93.9	95.7	93.9	0.0030	1.0548
K-Means	0	5.24	75.0	79.1	74.5	1.1976	0.1046
Logistic Regression	251	2.68	84.8	82.1	84.7	0.0085	0.0272
LSTM [48]	51,102	199.62	95.5	96.0	95.4	85.7291	0.2998
CNN-LSTM [48]	63,630	248.55	97.0	97.0	96.9	49.6258	3.7010
RNN [49]	232,658	908.82	96.9	96.3	96.0	226.0266	31.4683
Baseline 1D CNN [50]	8,439,426	32,190	99.3	99.0	98.5	854.8449	12.8933
SqueezeNet	354,370	1,401.85	54.5	55.0	39.7	191.7461	0.6807
EfficientNetB0	7,003,266	27,636.79	97.0	99.1	96.6	2,081.4195	186.4941
1D-MobileNetV1	3,167,554	12,392.10	49.0	51.9	32.8	1,475.6756	23.7306
ShuffleNetV1	753,578	3,062.25	48.5	44.8	44.5	106.2833	2.1184
CADNet	2,586	10.10	99.3	99.0	99.0	10.0856	0.3250

SqueezeNet, MobileNet, EfficientNet and ShuffleNet, are employed to evaluate performance on our subset, alongside our CADNet model. MobileNetV1 was modified to process one-dimensional ECG signals by replacing its two-dimensional convolutional layers with one-dimensional operations. Among the classical ML-based models, Gaussian Naive Bayes and Logistic Regression are highly efficient, with small sizes of 8.41 KB and 2.68 KB, minimal or no trainable parameters, and very low runtimes of 0.0039 and 0.0085 seconds, making them suitable for resource-constrained environments. Although KNN is relatively large at 353.66 KB and has no trainable parameters, it achieves a quick runtime of 0.0030 seconds. In contrast, K-Means, the smallest model at 5.24 KB, has a longer runtime of 1.1976 seconds, reflecting trade-offs between memory efficiency and computational speed across ML-based architectures. The KNN and LSTM models achieve the highest accuracy, at 93.9% and 95.5%, respectively. Gaussian Naive Bayes at 92.4% and Logistic Regression at 84.8% provide a favourable balance of accuracy and efficiency. Among the ML-based models, K-Means, with the lowest accuracy at 75.0%, demonstrates limited predictive capability. The baseline 1D-CNN exhibits the highest number of trainable parameters and the longest runtime among DL-based models, totalling 8,439,426 parameters and 854.844 seconds, which signifies the complexity of this model. Conversely, our CADNet stands out for its notably lighter parameter count, comprising only 2,586 parameters, thereby hinting at a more streamlined DL-based architectural design. Furthermore, LSTM, CNN-LSTM, and RNN also exhibit lower trainable parameter counts compared to the baseline 1D-CNN model. The sizes of the models display significant variability, with the baseline 1D-CNN being the largest, totalling 32,190 KB. In contrast, the CADNet is considerably smaller, occupying only 10.10 KB, while LSTM, CNN-LSTM, and RNN contain 199.62, 248.55, and 908.82 KB, respectively. The corresponding runtimes for these models are 85.7291 seconds for LSTM, 49.6258 seconds for CNN-LSTM, 226.0266 seconds for RNN, and 10.0856 seconds for the CADNet model, making our CADNet model particularly suitable for deployment in resource-constrained environments where memory limitations are a concern, as it is both significantly smaller in size and faster than other DL-based models. LSTM achieves an accuracy of 95.5%, which, while com-

mendable, represents the lowest performance within the group. Conversely, the CNN-LSTM model, integrating convolutional layers with LSTM layers, demonstrates a notable enhancement in accuracy, achieving 97.0%. RNN showcases an accuracy closely approximating that of the CNN-LSTM, at 96.9%. Both the baseline 1D-CNN and the CADNet achieve the highest accuracy at 99.3%, significantly surpassing the other DL-based models. This heightened level of accuracy suggests that both models excel in feature detection and classification, likely attributed to the robust capability of CNN in extracting crucial features indicative of CAD from ECG data. Additionally, this suggests that despite its simplicity, the CADNet does not compromise on predictive performance. To further demonstrate the suitability of the CADNet model for deployment in resource-limited environments, a well-known lightweight model is evaluated. The CADNet model exhibits only 2,586 trainable parameters and a runtime of 10.0856 seconds, achieving the highest accuracy at 99.3%. In contrast, EfficientNetB0, with over 7 million trainable parameters, achieves a high accuracy of 97% but requires a considerably longer runtime of 2,081.4195 seconds, highlighting its substantial demand for computational resources. SqueezeNet, 1D-MobileNetV1, and ShuffleNetV1, with 354,370, 3,167,554, and 753,578 trainable parameters, respectively, exhibit lower accuracy and extended runtimes of 106.2833 seconds, 1,475.6756 seconds, and 106.2833 seconds. These results highlight the CADNet model's advantage in achieving high performance with minimal computational resources.

To further evaluate computational efficiency, inference time is assessed to evaluate the suitability of each model for deployment in real-time and resource-constrained environments. The results indicate that traditional machine learning methods, including SVM, Gaussian Naive Bayes, Logistic Regression, and KNN, achieve the lowest inference times. Among ML-based methods, Gaussian Naive Bayes is the most efficient, requiring only 0.0419 ms per ECG signal. KNN is comparatively slower, averaging 1.0548 ms per ECG signal. Among DL-based models, the CNN-LSTM shows a good balance between prediction accuracy and speed, with an average inference time of 3.7010 ms per ECG signal. In comparison, the RNN takes longer, averaging 31.4683 ms per ECG signal, due to the extra processing required for handling sequences and its larger

number of trainable parameters. Lightweight DL-based architectures, such as SqueezeNet and ShuffleNet, show relatively fast inference times. In comparison, more complex models, including EfficientNetB0 and 1D-MobileNetV1, require much longer, with inference times of 186.4941 ms and 23.7306 ms per ECG signal, respectively. The proposed CADNet model achieves an inference time of only 0.3250 ms per ECG signal, while using just 2,586 trainable parameters, and still maintains a high level of classification accuracy. These results suggest that CADNet is well-suited for use in real-time or resource-constrained environments.

Figure 6 illustrates the comparative performance analysis between ML-based, DL-based, lightweight algorithms and our proposed lightweight model on CAD classification presented in Table III, including the CADNet model. Gaussian Naive Bayes, KNN, CNN-LSTM, RNN, and the CADNet model achieve high AUC and F1 values, demonstrating strong class separation and balanced precision-recall performance. With an AUC and F1 score of 99%, the CADNet model emerges as the top performer, making it highly suitable for CAD diagnosis requiring exceptional reliability and accuracy. SVM, K-Means, and Logistic Regression display moderate performance, with slightly lower AUC and F1 values, suggesting fair but less consistent precision-recall balance. In contrast, SqueezeNet, EfficientNetB0, MobileNetB0, and ShuffleNetV1 exhibit low AUC and F1 scores, indicating limited effectiveness in both class distinction and classification balance.

E. Generalisation and interpretability

Table IV illustrates the CADNet model trained using the PTB-XL database with a subset of 400 ECG signals: 200 CAD and 200 non-CAD. The model demonstrates high classification performance within the training dataset and robust generalisability across unseen subsets. Achieving a training accuracy of 95.90% and a test accuracy of 92.05% on the PTB-XL dataset, the model exhibits reliable learning and validation performance, as indicated by a precision of 96.35%, recall of 95.65%, and an F1 score of 96%. These results demonstrate the model's effectiveness in accurately identifying CAD and non-CAD cases. To further assess the model's generalisability, we conducted an initial validation on a subset of 200 ECG signals: 100 non-CAD signals from the Fantasia database and 100 CAD signals from the MIMIC III database. The model achieved a test accuracy of 87%, with a perfect recall of 100%, though with a slight reduction in precision to 74% on this validation set. The resulting F1 score of 85.06% indicates stable performance. Subsequently, we conducted a second validation on a subset of 200 ECG signals: 100 non-CAD ECG signals from the Fantasia database and 100 CAD ECG signals from the St. Petersburg database. The model achieved a test accuracy of 88%, recall of 100%, precision of 76%, and an F1 score of 86.36%. While the model demonstrates robust sensitivity for CAD detection across diverse datasets, the observed reduction in precision on validation subsets suggests a sensitivity-specificity trade-off that could benefit from further optimisation to enhance specificity and reduce false positives. This performance underscores the potential

of the CADNet model for CAD diagnosis, with scope for refinement to improve adaptability across varied ECG data sources.

Table V presents the CADNet model trained on ECG signals from the PTB-XL, MIMIC-III, and Fantasia databases, using a subset comprising 100 ECG signals from each database. The model achieved a training accuracy of 99.5% and a testing accuracy of 95.96%, demonstrating reliable performance in classifying CAD and non-CAD cases. The high precision of 99.29%, together with a perfect recall of 100%, suggests that the model accurately identifies CAD cases, with minimal risk of overlooking true positives, as reflected in an F1 score of 99.64%. This level of performance indicates that the model is highly proficient in distinguishing between CAD and non-CAD ECG signals, ensuring a balanced approach between sensitivity and specificity. The first validation subset consisted of 100 non-CAD ECG signals from the Fantasia database and 100 non-CAD ECG signals from the MIMIC-III database. The model's robustness was demonstrated, achieving a test accuracy of 99%. Precision slightly decreased to 98%, while recall remained perfect at 100%, resulting in an F1 score of 98.99%. This slight reduction in precision, alongside perfect recall, suggests occasional misclassification of non-CAD cases as CAD but consistent identification of all true CAD cases. Subsequently, the second validation subset was formed with 100 non-CAD ECG signals from the Fantasia database and 100 CAD ECG signals from the St. Petersburg database. The model continued to demonstrate high performance, achieving a test accuracy of 98.49%, with precision reaching 100% and recall at 95.08%, resulting in an F1 score of 97.48%. This level of precision indicates that all identified CAD cases are true positives.

To enhance interpretability, t-SNE analysis was performed to visualise high-dimensional data and examine the role of two key modules: feature encoding and compact pooling layers in distinguishing between the two classes as shown in Figure 7. ECG signals exhibit significant overlap in Figure 7a, indicating that the feature encoding layer is beginning to learn distinguishing features between the two classes. Although some overlap remains, a clearer boundary begins to emerge between non-CAD and CAD ECG signals, suggesting that the model is progressively capturing patterns that facilitate class separation as shown in Figure 7b. The compact pooling layer achieves near-complete separation of the two classes in the feature space, as shown in Figure 7c. This indicates that the model has effectively learned to differentiate between non-CAD and CAD samples. The distinct separation in this layer underscores that the features learned in this layer are highly effective at distinguishing between classes.

To evaluate the classification accuracy of the proposed model across diverse populations and assess its reliability for real-world clinical use, we validated the model trained in Table V across different age groups. ECG signals from the Fantasia and PTB-XL databases were used for this assessment, as presented in Table VI. As seen from this table, CADNet achieves the highest accuracy in the 40–50 age group at 98.83% and the lowest in the over 60 age group at 97.54%. Although the overall average accuracy is high at 98.23%, minor variations

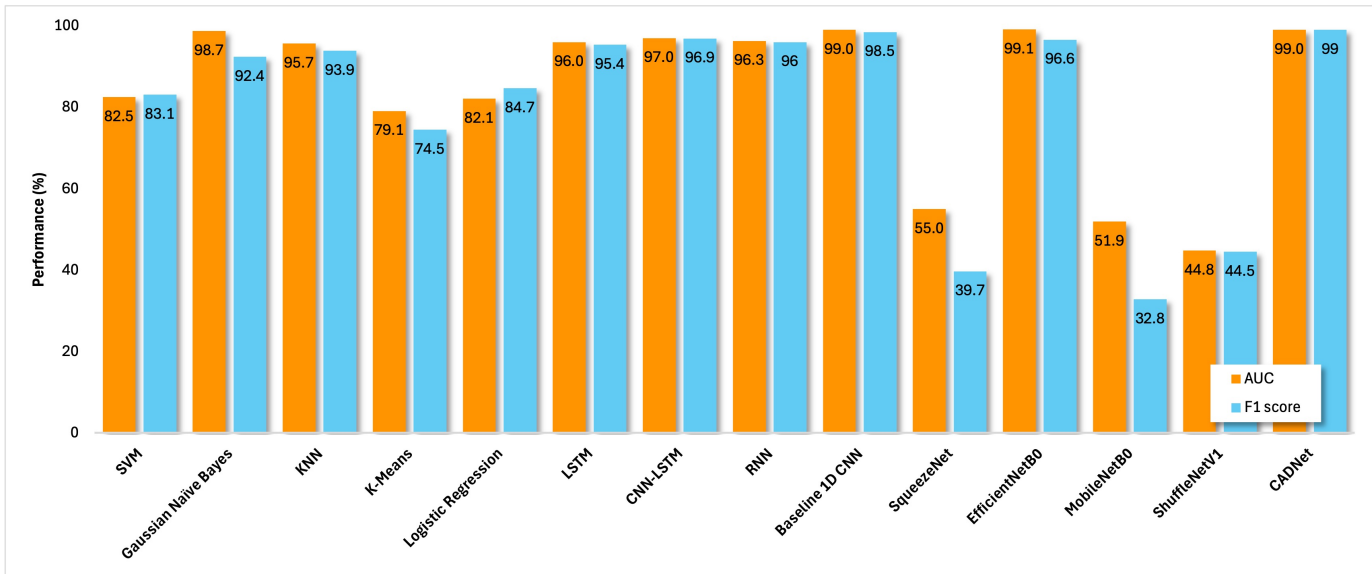


Fig. 6: Performance comparison of ML-based, DL-based, lightweight models, and our CADNet model using AUC and F1 metrics to assess class distinction and predictive effectiveness.

TABLE IV: Performance of the CADNet Model Trained with PTB-XL database.

Metric(s)	Train Accuracy	Test Accuracy	Precision	Recall	F1 Score
Trained with PTB-XL	0.9590	0.9205	0.9635	0.9565	0.9600
Test on Fantasia and MIMIC III	-	0.8700	0.7400	1.0000	0.8506
Test on Fantasia and St Peterburg	-	0.8800	0.7600	1.0000	0.8636

TABLE V: Performance of the CADNet Model Trained with PTB-XL, MIMIC III and Fantasia databases.

Metric(s)	Train Accuracy	Test Accuracy	Precision	Recall	F1 Score
Trained with Fantasia, MIMIC III and PTB-XL	0.9950	0.9596	0.9929	1.0000	0.9964
Test on Fantasia and MIMIC III	-	0.9900	0.9800	1.0000	0.9899
Test on Fantasia and St Peterburg	-	0.9849	1.0000	0.9508	0.9748

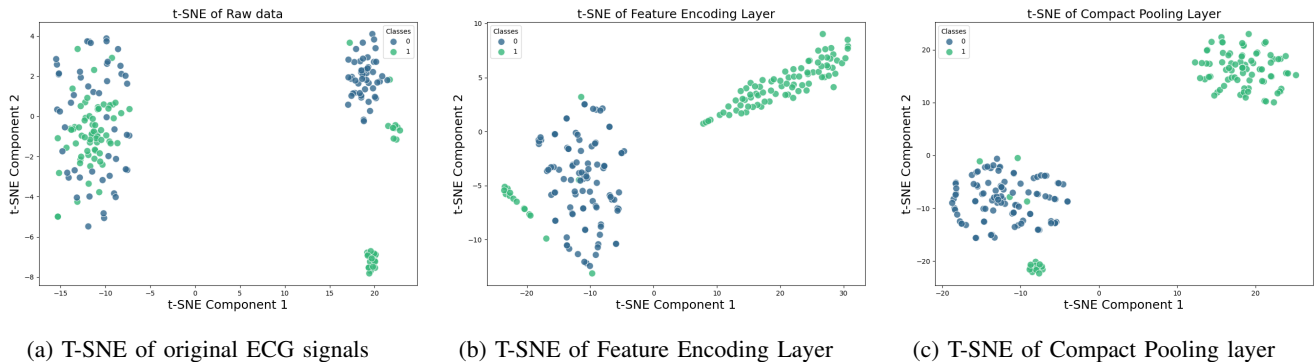


Fig. 7: T-SNE visualisation of the feature space, with class labels: 0 (Normal) and 1 (CAD).

are evident across different age groups. Notably, performance declines slightly in both the 10–20 and over 60 age groups, suggesting that the model may be slightly less effective at generalising to these demographics. This trend could reflect underlying physiological variations in ECG signals associated with age.

IV. LIMITATIONS AND FUTURE DIRECTIONS

One of the main limitations in CAD diagnosis using ECG signals is the limited availability of datasets, primarily due to the absence of clear medical indicators of CAD, such as single-vessel or multi-vessel disease. After a thorough exploration of publicly available datasets, we identified MIMIC-III, St. Pe-

TABLE VI: Test Accuracy Across Age Groups (Fantasia and PTB-XL Databases).

Age Group (Years)	Accuracy (%)
10 – 20	97.87
20 – 30	98.35
30 – 40	98.49
40 – 50	98.83
50 – 60	98.27
Over 60	97.54
Average	98.23

tersburg, and PTB-XL as suitable and comprehensive sources for evaluation. In future work, we aim to expand our research by classifying different types of CAD within the PTB-XL dataset. However, the results presented in this study, evaluated across four distinct datasets, provide strong validation of the model's effectiveness and generalizability.

Although the CADNet achieved high accuracy on multiple public datasets, these may not fully reflect real-world clinical variability. Factors such as device differences, recording conditions, and patient diversity can affect performance. While we considered this by testing across different age groups, further validation in real clinical settings is needed to confirm generalisability. Future work should consider evaluation on prospective datasets rather than relying solely on existing public datasets.

A promising direction for future research is the integration of explainable AI methods, such as ST-CNN-GAP-5 [51], to enhance the interpretability of CADNet's decisions. This approach would facilitate a deeper understanding of the model's reasoning and enable the generation of automated reports for clinical follow-ups.

While we focused on the superclass-level diagnostic categories to be able to use all four datasets simultaneously, analysing model performance at the subclass level could offer deeper insights into the model's discriminative ability across various CAD subtypes. Hence, subclass-level evaluation is a promising extension for future work to refine the model's clinical applicability further.

Additionally, further studies could explore the use of multiple ECG leads to gain deeper insights into CAD-related ECG patterns. We also plan to deploy CADNet on resource-constrained devices, such as the STM32F469I-DISCO, to assess its performance in limited environments, focusing on power consumption and real-time runtime efficiency.

V. CONCLUSION

Our study introduced the CADNet model to differentiate between cases of CAD and non-CAD, to reduce the complexity of the model and facilitate its deployment on resource-constrained devices. Through the utilisation of data acquired from PhysioNet, our findings demonstrated the model's capability to independently classify these binary classes while maintaining its simplicity. The performance of the CADNet

which averaged 99.3% accuracy with 2,586 trainable parameters, surpassed that of other classical machine learning, DL-based and lightweight models, highlighting the reduction in computational resources or complexity without compromising predictive performance. The code used to implement the proposed method is available from the corresponding author upon reasonable request.

VI. REFERENCES

- [1] N. Ramya, V. Prabakaran, A. Abbas, and S. P. Shankar, "Study on risk factors and angiographic pattern of coronary artery involvement in patients presenting with angina," *Int J Adv Med*, vol. 6, p. 232, 2019.
- [2] A. H. Abdelaziz, G. F. Gomaa, and A. M. Algamal, "Treatment strategies for patients with obstructive coronary artery disease (limited mansoura university experience) in 2021," *The Egyptian Journal of Hospital Medicine*, vol. 91, no. 1, pp. 5003–5008, 2023.
- [3] Who.int., "Cardiovascular diseases," <https://www.who.int/health-topics/cardiovascular-diseases/#tab=tab.1>, 2023.
- [4] Who.int., "Cardiovascular diseases (cvds)," [https://www.who.int/news-room/fact-sheets/detail/cardiovascular-diseases-\(cvds\)](https://www.who.int/news-room/fact-sheets/detail/cardiovascular-diseases-(cvds)), 2019.
- [5] I. Zeljković, H. Pintarić, M. Vrsalović, and I. Kruljac, "Effectiveness of cardiogoniometry compared with exercise-ecg test in diagnosing stable coronary artery disease in women," *QJM: An International Journal of Medicine*, vol. 110, no. 2, pp. 89–95, 2017.
- [6] M. Dey, N. Omar, and M. A. Ullah, "Temporal feature-based classification into myocardial infarction and other cvds merging cnn and bi-lstm from ecg signal," *IEEE Sensors Journal*, vol. 21, no. 19, pp. 21 688–21 695, 2021.
- [7] V. Jahmunah, E. Y. K. Ng, T. R. San, and U. R. Acharya, "Automated detection of coronary artery disease, myocardial infarction and congestive heart failure using gaborenn model with ecg signals," *Computers in biology and medicine*, vol. 134, p. 104457, 2021.
- [8] R. Banerjee, A. Ghose, and K. Muthana Mandana, "A hybrid cnn-lstm architecture for detection of coronary artery disease from ecg," in *2020 International Joint Conference on Neural Networks (IJCNN)*, 2020, pp. 1–8.
- [9] A. D. Dolatabadi, S. E. Z. Khadem, and B. M. Asl, "Automated diagnosis of coronary artery disease (cad) patients using optimized svm," *Computer methods and programs in biomedicine*, vol. 138, pp. 117–126, 2017.
- [10] G. G. Geweid and J. D. Chen, "Automatic classification of atrial fibrillation from short single-lead ecg recordings using a hybrid approach of dual support vector machine," *Expert Systems with Applications*, vol. 198, p. 116848, 2022.
- [11] Q. H. Nguyen, B. P. Nguyen, T. B. Nguyen, T. T. Do, J. F. Mbinta, and C. R. Simpson, "Stacking segment-based cnn with svm for recognition of atrial fibrillation from single-lead ecg recordings," *Biomedical Signal Processing and Control*, vol. 68, p. 102672, 2021.
- [12] M. Deng, L. Qiu, H. Wang, W. Shi, and L. Wang, "Atrial fibrillation classification using convolutional neural networks and time domain features of ecg sequence," in *2020 IEEE 19th International Conference on Trust, Security and Privacy in Computing and Communications (TrustCom)*, 2020, pp. 1481–1485.
- [13] E. H. Houssein, I. E. Ibrahim, N. Neggaz, M. Hassaballah, and Y. M. Wazery, "An efficient ecg arrhythmia classification method based on manta ray foraging optimization," *Expert systems with applications*, vol. 181, p. 115131, 2021.
- [14] M. Naz, J. H. Shah, M. A. Khan, M. Sharif, M. Raza, and R. Damaševičius, "From ecg signals to images: a transformation based approach for deep learning," *PeerJ Computer Science*, vol. 7, p. e386, 2021.
- [15] S. Celin and K. Vasanth, "A novel method for ecg classification using polynomial based curve fitting," in *2019 IEEE International Conference on Electrical, Computer and Communication Technologies (ICEECT)*, 2019, pp. 1–9.
- [16] Z. Wang, L. Qian, C. Han, and L. Shi, "Application of multi-feature fusion and random forests to the automated detection of myocardial infarction," *Cognitive Systems Research*, vol. 59, pp. 15–26, 2020.
- [17] M. Hammad, A. M. Iliyasa, A. Subasi, E. S. Ho, and A. A. Abd El-Latif, "A multitier deep learning model for arrhythmia detection," *IEEE Transactions on Instrumentation and Measurement*, vol. 70, pp. 1–9, 2020.

- [18] V. Mazaheri and H. Khodadadi, "Heart arrhythmia diagnosis based on the combination of morphological, frequency and nonlinear features of ecg signals and metaheuristic feature selection algorithm," *Expert Systems with Applications*, vol. 161, p. 113697, 2020.
- [19] S. K. Bashar, E. Ding, D. Albuquerque, M. Winter, S. Binici, A. J. Walkey, D. D. McManus, and K. H. Chon, "Atrial fibrillation detection in icu patients: A pilot study on mimic iii data," in *2019 41st Annual International Conference of the IEEE Engineering in Medicine and Biology Society (EMBC)*, 2019, pp. 298–301.
- [20] M. U. Khan, S. Aziz, S. Z. Hassan Naqvi, and A. Rehman, "Classification of coronary artery diseases using electrocardiogram signals," in *2020 International Conference on Emerging Trends in Smart Technologies (ICETST)*, 2020, pp. 1–5.
- [21] W. Yang, Y. Si, D. Wang, G. Zhang, X. Liu, and L. Li, "Automated inpatient and inter-patient coronary artery disease and congestive heart failure detection using efp-net," *Knowledge-Based Systems*, vol. 201, p. 106083, 2020.
- [22] S. Singh, S. K. Pandey, U. Pawar, and R. R. Janghel, "Classification of ecg arrhythmia using recurrent neural networks," *Procedia computer science*, vol. 132, pp. 1290–1297, 2018.
- [23] L. Yao, C. Liu, P. Li, J. Wang, Y. Liu, W. Li, X. Wang, H. Li, and H. Zhang, "Enhanced automated diagnosis of coronary artery disease using features extracted from qt interval time series and st-t waveform," *IEEE Access*, vol. 8, pp. 129 510–129 524, 2020.
- [24] J. H. Tan, Y. Hagiwara, W. Pang, I. Lim, S. L. Oh, M. Adam, R. S. Tan, M. Chen, and U. R. Acharya, "Application of stacked convolutional and long short-term memory network for accurate identification of cad ecg signals," *Computers in Biology and Medicine*, vol. 94, pp. 19–26, 2018.
- [25] Y. Guo, D. Zhou, X. Ruan, and J. Cao, "Variational gated autoencoder-based feature extraction model for inferring disease-mirna associations based on multiview features," *Neural Networks*, vol. 165, pp. 491–505, 2023.
- [26] A. K. Singh and S. Krishnan, "Ecg signal feature extraction trends in methods and applications," *BioMedical Engineering OnLine*, vol. 22, no. 1, p. 22, 2023.
- [27] H. Mewada, "2d-wavelet encoded deep cnn for image-based ecg classification," *Multimedia Tools Appl.*, vol. 82, no. 13, p. 20553–20569, Jan. 2023.
- [28] F. DW, D. TG, A. YM, K. SR, and A. TF, "Lightweight multireceptive field cnn for 12-lead ecg signal classification," *Computational Intelligence and Neuroscience*, vol. 2022, p. 8413294, 2022.
- [29] H. Mewada and I. M. Pires, "Electrocardiogram signal classification using lightweight dnn for mobile devices," *Procedia Computer Science*, vol. 224, pp. 558–564, 2023, 18th International Conference on Future Networks and Communications / 20th International Conference on Mobile Systems and Pervasive Computing / 13th International Conference on Sustainable Energy Information Technology.
- [30] K. Qin, W. Huang, T. Zhang, H. Zhang, and X. Cheng, "A lightweight selfonn model for general ecg classification with pretraining," *Biomedical Signal Processing and Control*, vol. 89, p. 105780, 2024.
- [31] Y. Cao, T. Wei, B. Zhang, N. Lin, J. J. Rodrigues, J. Li, and D. Zhang, "MI-net: Multi-channel lightweight network for detecting myocardial infarction," *IEEE Journal of Biomedical and Health Informatics*, vol. 25, no. 10, pp. 3721–3731, 2021.
- [32] N. Rahuja and S. K. Valluru, "A comparative analysis of deep neural network models using transfer learning for electrocardiogram signal classification," in *2021 International Conference on Recent Trends on Electronics, Information, Communication & Technology (RTEICT)*, 2021, pp. 285–290.
- [33] N. Nonaka and J. Seita, "Electrocardiogram classification by modified efficientnet with data augmentation," in *2020 Computing in Cardiology*, 2020, pp. 1–4.
- [34] M. Tang, Y. Fan, J. Huang, P. Gao, and Y. Zhan, "Classification of arrhythmia based on the fusion of mobilenet and bilstm models," in *2023 15th International Conference on Intelligent Human-Machine Systems and Cybernetics (IHMSC)*, 2023, pp. 45–48.
- [35] H. Tesfai, H. Saleh, M. Al-Qutayri, M. B. Mohammad, T. Tekeste, A. Khandoker, and B. Mohammad, "Lightweight shufflenet based cnn for arrhythmia classification," *IEEE Access*, vol. 10, pp. 111 842–111 854, 2022.
- [36] J. Xiao, J. Liu, H. Yang, Q. Liu, N. Wang, Z. Zhu, Y. Chen, Y. Long, L. Chang, L. Zhou, and J. Zhou, "Ulegcnet: An ultra-lightweight end-to-end ecg classification neural network," *IEEE Journal of Biomedical and Health Informatics*, vol. 26, no. 1, pp. 206–217, 2022.
- [37] A. E. Johnson, T. J. Pollard, L. Shen, L.-w. H. Lehman, M. Feng, M. Ghassemi, B. Moody, P. Szolovits, L. Anthony Celi, and R. G. Mark, "Mimic-iii, a freely accessible critical care database," *Scientific data*, vol. 3, no. 1, pp. 1–9, 2016.
- [38] A. L. Goldberger, L. A. Amaral, L. Glass, J. M. Hausdorff, P. C. Ivanov, R. G. Mark, J. E. Mietus, G. B. Moody, C.-K. Peng, and H. E. Stanley, "Physiobank, physiotoolkit, and physionet: components of a new research resource for complex physiologic signals," *circulation*, vol. 101, no. 23, pp. e215–e220, 2000.
- [39] P. Wagner, N. Strodthoff, R.-D. Bousseljot, D. Kreiseler, F. I. Lunze, W. Samek, and T. Schaeffter, "Ptb-xl, a large publicly available electrocardiography dataset," *Scientific data*, vol. 7, no. 1, pp. 1–15, 2020.
- [40] N. Iyengar, C. Peng, R. Morin, A. L. Goldberger, and L. A. Lipsitz, "Age-related alterations in the fractal scaling of cardiac interbeat interval dynamics," *American Journal of Physiology-Regulatory, Integrative and Comparative Physiology*, vol. 271, no. 4, pp. R1078–R1084, 1996.
- [41] M. Sharma and U. R. Acharya, "A new method to identify coronary artery disease with ecg signals and time-frequency concentrated antisymmetric biorthogonal wavelet filter bank," *Pattern Recognition Letters*, vol. 125, pp. 235–240, 2019.
- [42] E. Butun, O. Yildirim, M. Talo, R.-S. Tan, and U. R. Acharya, "1d-cadcapsnet: One dimensional deep capsule networks for coronary artery disease detection using ecg signals," *Physica Medica*, vol. 70, pp. 39–48, 2020.
- [43] U. R. Acharya, H. Fujita, O. S. Lih, M. Adam, J. H. Tan, and C. K. Chua, "Automated detection of coronary artery disease using different durations of ecg segments with convolutional neural network," *Knowledge-Based Systems*, vol. 132, pp. 62–71, 2017.
- [44] R. Holgado-Cuadrado, C. Plaza-Seco, L. Lovisolo, and M. Blanco-Velasco, "Characterization of noise in long-term ecg monitoring with machine learning based on clinical criteria," *Medical & Biological Engineering & Computing*, pp. 1–14, 2023.
- [45] H. Ghonchi, S. Ferdowsi, and V. Abolghasemi, "Common spatial pattern with deep learning for fetal heart rate monitoring," in *2022 IEEE Workshop on Signal Processing Systems (SiPS)*, 2022, pp. 1–6.
- [46] J. S. Richman and J. R. Moorman, "Physiological time-series analysis using approximate entropy and sample entropy," *American journal of physiology-heart and circulatory physiology*, vol. 278, no. 6, pp. H2039–H2049, 2000.
- [47] R. Alcaraz, D. Abásolo, R. Hornero, and J. J. Rieta, "Optimal parameters study for sample entropy-based atrial fibrillation organization analysis," *Computer methods and programs in biomedicine*, vol. 99, no. 1, pp. 124–132, 2010.
- [48] Y. Obeidat and A. M. Alqudah, "A hybrid lightweight 1d cnn-lstm architecture for automated ecg beat-wise classification," *Traitement du Signal*, vol. 38, no. 5, 2021.
- [49] D. Fernandes, "Ecg time-series classification." [Online]. Available: <https://github.com/dave-fernandes/ECGClassifier>
- [50] A. Phoemsuk and V. Abolghasemi, "Coronary artery disease classification using one-dimensional convolutional neural network," in *2024 IEEE Conference on Artificial Intelligence (CAI)*, 2024.
- [51] A. Anand, T. Kadian, M. K. Shetty, and A. Gupta, "Explainable ai decision model for ecg data of cardiac disorders," *Biomedical Signal Processing and Control*, vol. 75, p. 103584, 2022.